

Synthesis and Characterizations of TiO₂/Ag Photoanodes for used Indigo Carmine Sensitizer Based Solar Cells

Soner Çakar^{1,2,3*}, Keziban Atacan⁴, Nuray Güy²

¹Zonguldak Bulent Ecevit University, Science & Arts Faculty, Department of Chemistry, Zonguldak, Turkey.

²Sakarya University, Science & Arts Faculty, Department of Chemistry, Sakarya, Turkey

³Zonguldak Bulent Ecevit University, Science and Technology Research and Application Center (ARTMER), Zonguldak, Turkey.

⁴Sakarya University, Biomedical, Magnetic, Semiconductor Materials Application and Research Center (BIMAS-RC), Sakarya, Turkey.

*cakarsoner@gmail.com

Received: 04 June 2018

Accepted: 23 January 2019

DOI: 10.18466/cbayarfbe.430644

Abstract

In this work we have prepared Ag doped TiO₂ composite semiconductor by microwave hydrothermal methods. The prepared TiO₂/Ag photoanode was characterized via XRD, FE-SEM and DRS spectroscopy techniques. Then this composite was used as a photoanode material for dye sensitized solar cells. The TiO₂/Ag photoanode was prepared by spin coating technique. The sensitizer of this solar cell is indigo carmine and it was prepared in different pH solution in ACN. The higher solar cell efficiency values were achieved up to 1.91% with TiO₂/Ag photoanode and in pH 5.3 indigo carmine dye solution. As a result, in this study, it was observed that the addition of Ag nanoparticles was increased the efficiency of solar cell by 20-45%.

Keywords: Dye sensitized solar cells, indigo carmine, TiO₂/Ag.

1. Introduction

Dye sensitized solar cells (DSSCs) has been regarded as a third generation solar cell [1], they paid attention to important class of photovoltaic cells [2]. Nowadays, DSSCs have been the subject of many studies related to solar cells due to their low cost, facile fabrication, and environmental friendly behavior. Typically, DSSCs have four main components as following; large band gap semiconductor coated photoanode, light sensitive sensitizers, redox couple electrolyte, and counter electrode. In recent decade due to the harmful effects of dyes and solvents used in DSSCs, reports have been enormously used the environmental friendly materials in DSSCs [3]. For this reason, the use of environmentally friendly natural dyes, which do not contain noble metals, are increasing day by day. These dyes are examined in three main categories as following; i) metal complexes dyes, ii) organic dyes and iii) natural dyes [4, 5] Different natural dyes have been used as sensitizers in DSSCs, for example chlorophyll, carotene, anthocyanin, and tannin [6, 7].

Indigo carmine (disodium;(2E)-3-oxo-2-(3-oxo-5-sulfonato-1H-indol-2-ylidene)-1H-indole-5-sulfonate) is an

organic salt, purple solid and soluble in water. It is also natural organic dye and widely used in many industrial applications like textiles, printing, dyeing and food. Indigo carmine is derived from indigo dye. Indigo is one of the important dye groups for textile industry because blue dyes were found seldomly in the past. [8, 9]. The indigo carmine structure is shown in Fig 1.

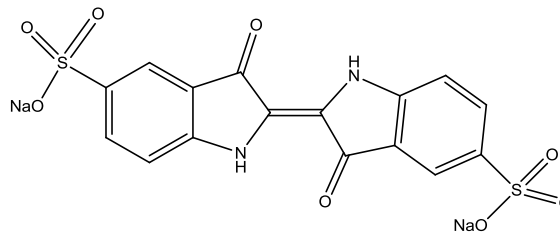


Figure 1. Indigocarmine structure.

TiO₂ is an encouraging material and mainly used photoanode material in DSSCs. It has unique properties in DSSCs such as low toxicity, excellent electron transport and good chemical stability. Also, it has several potential applications for gas sensor, lithium ion batteries and photocatalysis [10–12]. In DSSCs, several semiconductors (ZnO,

SnO₂, etc.) have been used as an alternative for the TiO₂. TiO₂ consist in three crystalline forms; rutile, anatase and brookite. The anatase form of TiO₂ is the most suitable polymorphs because of their unique charge transport property. The rutile is the most stable thermodynamic polymorph of TiO₂ at all temperatures. Therefore, anatase TiO₂ crystallization depends on preparation conditions and temperature [13,14]. TiO₂ is widely used as photoanode materials for DSSC applications. The potential advantages of TiO₂ are the chemical stability, high electron mobility and environmentally friendliness etc. The Ag nanoparticles have several application as catalysis, enzyme immobilizations, solar cells etc. The Ag nanoparticles have accelerated electron mobility.

In this study, we have prepared TiO₂/Ag nanocomposite semiconductor electrode and it can be used dye sensitized solar cells. The TiO₂/Ag nanocomposite were prepared microwave assisted hydrothermal procedure. Then these composites were characterized X-ray diffractometry (XRD), field emission-scanning electron microscopy (FE-SEM), energy dispersive X-ray analysis (EDS) and diffused reflectance spectroscopy (DRS) spectra. The indigo carmine dyes were used as the solar cells. The indigo carmine solution with different pH values were prepared in water and characterized by cyclic voltammetry (CV) and UV-Vis techniques. As investigated solar cells were prepared using this dye and TiO₂/Ag photoanode, traditional Pt counter electrode and iodide/triiodide electrolyte. The current density voltage curves were performed via electrochemical workstation (CHI 660C) under the solar simulator (Oriol LCS-100).

2. Materials and Methods

2.1 Materials

Indigo carmine (C₁₆H₈N₂Na₂O₈S₂), titanium isopropoxide (C₁₂H₂₈O₄Ti), silver nitrate (AgNO₃), potassium hydroxide (KOH), ethyl cellulose, 2-propanol, fluorinated tin oxide glass (FTO glass, 7 Ω/sq.), 4-tert butylpyridine were purchased from Sigma Aldrich. Iodine (I₂) was attained from Riedel de Haen. Dihydrogen hexachloroplatinate (IV) hexahydrate (H₂PtCl₆.6H₂O) was obtained from Alfa Aesar. All materials were analytical grade and used as received without further treatment.

2.2 TiO₂/Ag nanocomposite synthesis

TiO₂/Ag nanocomposite were synthesized via microwave hydrothermal synthesis methods. The 5 mL titanium isopropoxide (17 mmol) and 0.17 g AgNO₃ (1mmol) were dissolved 60 mL deionized water and transferred Teflon lined microwave hydrothermal cup. This solution was vigorously stirred under magnetic stirrer at 30 min. Then the 1.3 g KOH was added this solution and stirred with a magnetic stirrer at 30 min. The microwave radiation, temperature and time are settled 380W, 100°C and 1h, respectively. The grey

product was centrifuged and washed with ultrapure water and ethanol three times. Then, the TiO₂/Ag nanocomposite was dried 60°C for 12h. To compare all samples, TiO₂ nanoparticles were synthesis using similar procedure.

2.3. Different pH of indigo carmine solution preparation

10mM indigo carmine solution was prepared in 50 mL ultrapure water. The pH of this solution was selected as 5.3. For the comparison, the pH values 11.5 and 14 indigo carmine solutions were performed using 0.1M KOH. Indigo carmine is redox indicator and its solution is blue at the pH range of 0-11, but its color is changed to yellow at pH range of 11-14. Therefore, in this study indigo carmine solutions were prepared in three different pH values for solar cell applications.

2.4. Solar cell fabrication

The photoanode films were coated on the fluoride doped tin oxide (FTO) conductive glass by spin coating technique. The viscous paste, which includes TiO₂ or TiO₂/Ag nanocomposite and ethyl cellulose were elaborated and coated on FTO glass and sintered at 450°C at 30 min. The TiO₂ or TiO₂/Ag photoanodes were immersed in a 10 mM dye sensitizer solution for 24 h in the dark. The performed counter electrode was used as; a one drop 5 mM H₂PtCl₆.6H₂O solution spreading on FTO glass. The counter electrode was sintered at 450°C for 30 min. The electrolyte solution was prepared using of 0.1 M LiI, 0.05 M I₂ and 0.5 M 4-tert-butylpyridine in acetonitrile. The solar cells assembly were sandwiched and clipped together with photoanode and counter electrodes. The electrolyte solution was injected into the internal space of the cells.

3. Results and Discussion

3.1 TiO₂/Ag nanocomposite

The XRD spectra of the TiO₂ and TiO₂/Ag nanocomposite were shown in Fig 2. The small amount of the Ag nanoparticles was added to the TiO₂ anatase structure does not deformation. The calculated values of TiO₂ and TiO₂/Ag samples are given in Table 1. The lattice strain and crystallite size were performed from using X'Pert High Score Plus software;

$$D = \frac{0.89\lambda}{\beta \cos\theta} \quad \beta = \beta_{obs} - \beta_{std} \quad (1)$$

$$\varepsilon = \frac{\beta}{4 \tan \theta} \quad \beta = \sqrt{(\beta_{obs}^2 - \beta_{std}^2)} \quad (2)$$

Where ε is the lattice strain, λ is the X-ray wavelength angular line, D is crystalline size, β is full width at half maximum (FWHM) and θ is the Bragg's angle. The achieved crystalline size of TiO₂ and TiO₂/Ag are 25.4 and 65.7 nm, respectively. The achieved strain of TiO₂ and TiO₂/Ag are 0.64 and 0.46 %, respectively. The differences between both crystalline size and strain values of prepared TiO₂ and

TiO₂/Ag samples can be explained that, when the Ag is asserted in the system, the TiO₂ anatase lattice can be expanded and this expansion mechanism can be raises the crystalline size.

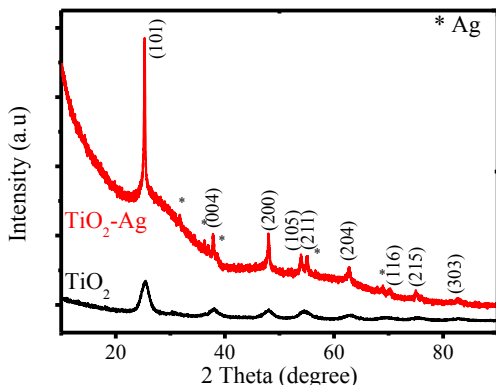


Figure 2. XRD patterns of TiO₂ and TiO₂/Ag.

Table 1. Crystalline properties for TiO₂ and TiO₂/Ag

Photoanode	Lattice Parameters		Volume (Å) ³	Crystalline size (nm)	Micro Strain (%)
	a (Å)	c (Å)			
TiO ₂	3.804	9.391	135.89	25.4	0.64
TiO ₂ /Ag	3.814	9.415	135.94	65.7	0.46

The FE-SEM images and EDS spectra of TiO₂/Ag nanocomposite are shown in Fig 3. As seen in Fig. 3, the small Ag nanoparticles for doped TiO₂ surface for uniform distribution. The EDS spectra demonstrated that the TiO₂ structure were doped with Ag ions, and Ag nanoparticles has deposited on TiO₂. Also, the weight percent and atomic percent of the Ag nanoparticles were found to be 0.10 and 0.02%, respectively. This small Ag nanoparticles were accelerated electron mobility and could be improved the solar cells efficiency. In this study, the DRS spectra of the both TiO₂ and TiO₂/Ag nanocomposite were taken and the band gap values of these samples were compared. The DRS results shown that the TiO₂/Ag nanocomposite absorbed more light in all region of UV-Vis compared to TiO₂. This is probably due to the Ag nanoparticles, because the color of TiO₂/Ag nanocomposite is grey. It was also decreased the light reflection. The band gap values of the TiO₂/Ag nanocomposite and TiO₂ were calculated using Kubelka-Munk equation and the detailed calculation can be seen in the previous study [15]. According to this study the band gap values of the TiO₂ are 3.17 and 3.22 eV, respectively. The band gap values of anatase TiO₂ is 3.2 eV. The band gap values of both TiO₂ and TiO₂/Ag nanocomposite are suitable for the dye sensitized solar cell applications.

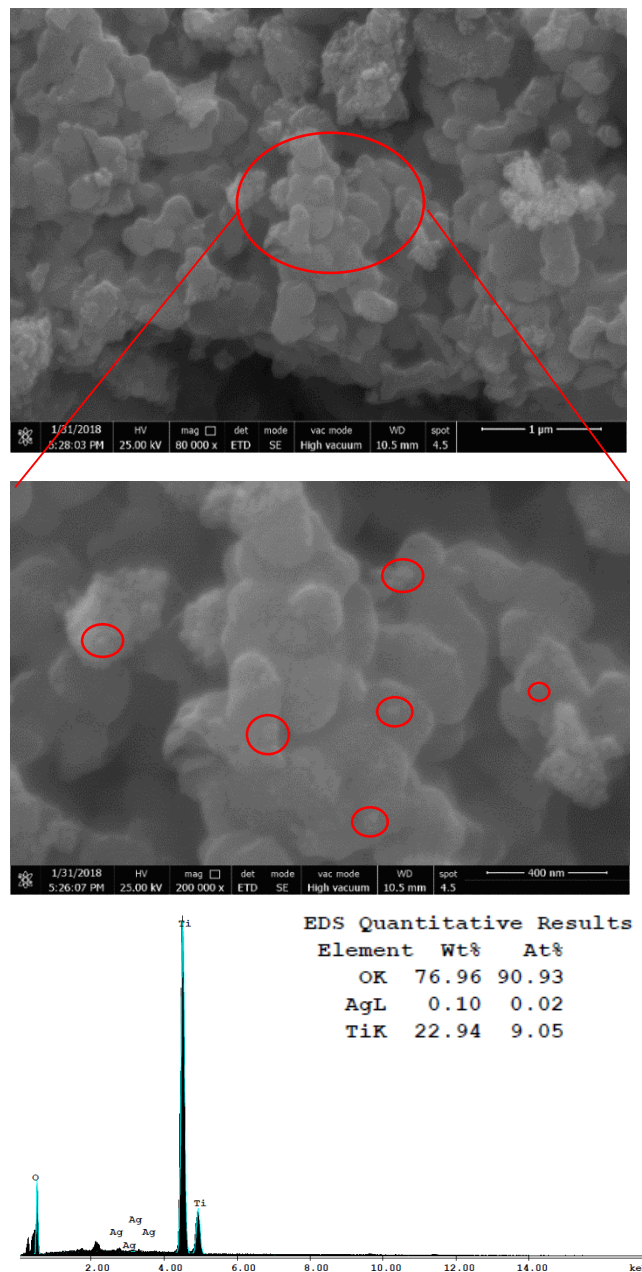


Figure 3. FE-SEM images and EDS spectra of TiO₂/Ag samples.

3.2. Indigo carmine

The 10 mM indigo carmine redox indicator solution were prepared at different pH values (5.3, 11 and 14) using ultrapure water. These pH values were selected, due to the color of indigo carmine changes at these pHs value. These dyes were characterized by cyclic voltammetry and UV-Vis techniques. The UV-Vis absorption spectra of these dyes were shown in Fig 5. It is seen that, the absorbance of these

solutions were decreased, while the pH values of dye solutions were increased. The both UV and Vis region light absorption of indigo carmine is higher at natural pH (5.3) than basic pH values. The light absorption of indigo carmine occurs at both 200-375 and 500-700 nm regions.

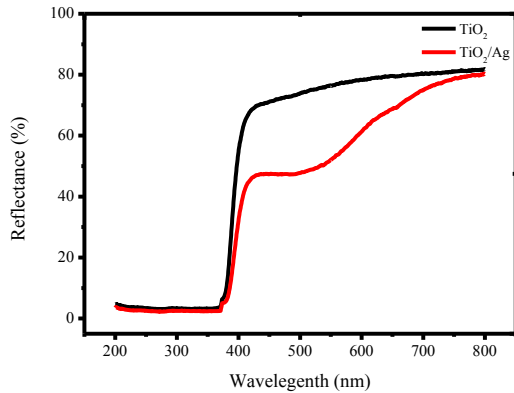


Figure 4. DRS spectra of TiO₂ and TiO₂/Ag samples.

The cyclic voltammetry curves of indigo carmine at different pH values are shown in Fig. 6. The HOMO and LUMO molecular orbital levels can be calculated in following equations [9,16];

$$E_{HOMO} = -e(E_{ox} + 4.40) eV \quad (3)$$

$$E_{LUMO} = -e(E_{red} + 4.40) eV \quad (4)$$

$$E_g = E_{LUMO} - E_{HOMO} \quad (5)$$

where E_{HOMO} is the HOMO orbital energy, E_{LUMO} is the LUMO orbital energy, E_{ox} is the first oxidation potential, E_{red} is the first reduction potential and E_g is the band gap energy. The Ferrocene/Ferrocenium is used as an internal standard for CV measurement. The estimated LUMO and HOMO levels of indigo carmine at different pH values (5.3, 11 and 14) are -5.08/-3.97, -5.12/-3.84 and -5.26/-3.71 eV, respectively. The HOMO, LUMO and E_g values of different pH conditions indigo carmine dye is summarized in Table 2. Additionally, the CV curves show that, the first oxidation peak is slightly decreased when the pH values are increased. The all dyes which have different pH values were suitable for the DSSCs applications. The LUMO molecular orbital level is so important in the dye sensitized solar cell study, due to the electron injection of the semiconductor conduction band. The conduction band of the TiO₂ is -4.00 eV. When the LUMO band of dyes are very close the TiO₂ conduction band, the more electron can be moved the conduction band. The LUMO band gap value of indigo carmine solution at pH 5.3 is close to the conduction band of TiO₂ and we predicted that this dye has higher solar cell performance. The UV-Vis absorption spectrum of this dye is also support this prediction.

Table 2. Electrochemical parameters of different pH solutions of indigo carmine

pH	E _{ox} (NHE)	E _{red} (NHE)	HOMO (eV)	LUMO (eV)	E _g
5.3	0.68	-0.43	-3.97	-5.08	1.11
11	0.72	-0.56	-3.84	-5.12	1.28
14	0.86	-0.69	-3.71	-5.26	1.55

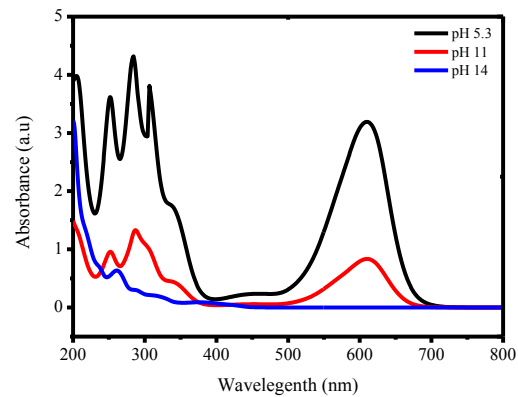


Figure 5. The UV-Vis absorbance spectra of indigo carmine at different pH values.

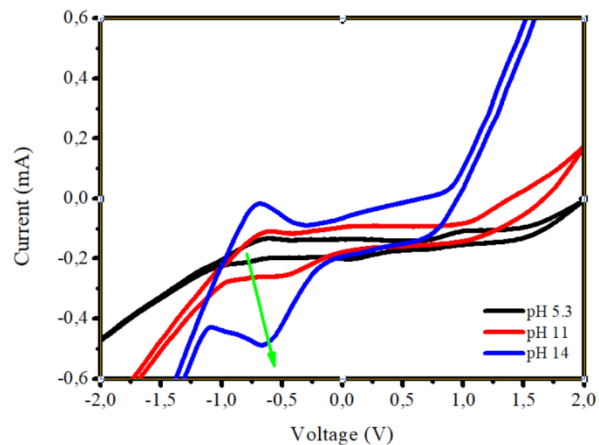


Figure 6. Cyclic voltammetry curves of indigo carmine at different pH values.

3.3. Solar Cells

To investigate the effect of Ag nanoparticles on indigo carmine based dye sensitized solar cells, series devices were prepared with both TiO₂ and TiO₂/Ag photoanodes. All parameters of fabricated DSSCs can be calculated using following equations;

$$FF = \frac{J_m \times V_m}{J_{sc} \times V_{oc}} \quad (6)$$

$$\eta = \frac{J_{sc} \times V_{oc} \times FF}{P_{in}} \quad (7)$$

where η is the solar cell efficiency, V_{oc} is the open circuit potential, J_{sc} is the short current density, J_m and V_m are the maximum current and voltage, respectively. P_{in} is the power of light source (AM 1.5).

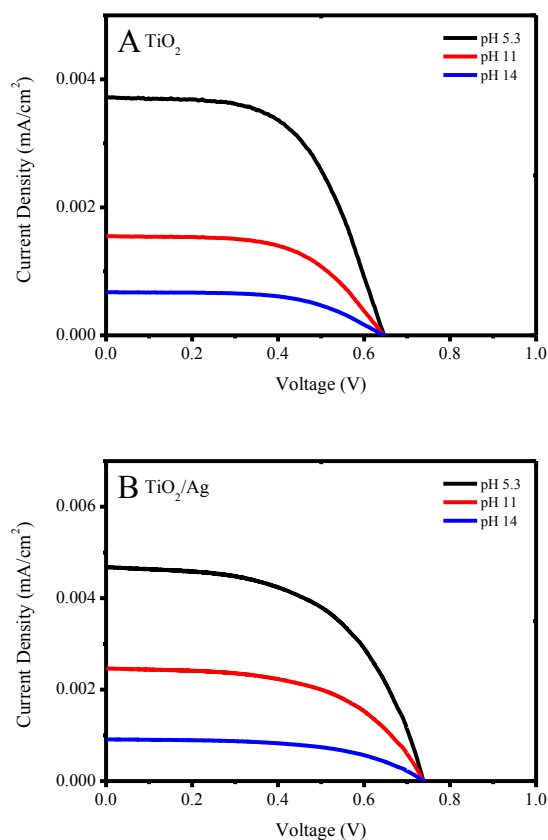


Figure 7. Current density voltage curves (J-V) of A) TiO₂ and B) TiO₂/Ag photoanodes for indigo carmine sensitizers at different pH value.

Table 3. Photovoltaic parameters of TiO₂ and TiO₂/Ag nanocomposite for indigo carmine at different pH values

	pH	J_{sc} (mA/cm ²)	V_{oc} (V)	FF (%)	η (%)
TiO ₂	5.3	3.71	0.65	57	1.38
	11	1.54	0.65	58	0.57
	14	0.67	0.63	59	0.25
TiO ₂ /Ag	5.3	4.69	0.74	55	1.91
	11	2.47	0.74	54	1.01
	14	0.91	0.73	56	0.37

The current density-voltage curves (J-V) of all prepared cells are exhibited in Fig 7 and the calculated solar cell parameters of these systems are listed in Table 3. The results indicated that the Ag nanoparticles is improved the solar cell efficiency. Hence, the solar cell efficiency value of the TiO₂ and indigo carmine at pH 5.3 was found to be 1.38%, and this value is lower than TiO₂/Ag nanocomposite photoanode based cells (1.91%). Additionally, the short circuit

current density (J_{sc}) and the open circuit voltage (V_{oc}) values were slightly increased for TiO₂/Ag nanocomposite compared with TiO₂ photoanodes. These values are influenced by the electron mobility. V_{oc} is also correlated with the TiO₂ conduction band and enhancement of charge recombination at the TiO₂/dye/electrolyte interface. The small doped Ag nanoparticles can be improved the electron mobility and can be improved the solar cell efficiency. When compared the solar cell efficiency values of TiO₂ and TiO₂/Ag, the Ag used in the photo anodes was increased the solar cell efficiency values by 20-45%.

4. Conclusion

The TiO₂ and TiO₂/Ag nanocomposite were prepared via microwave assisted hydrothermal methods and characterized via XRD, FE-SEM and DRS. The indigo carmine at different pH values are prepared in ultrapure water and characterized by UV-Vis and CV techniques. The TiO₂ or TiO₂/Ag photoanodes were prepared by spin coating technique. The dye sensitized solar cells were fabricated by TiO₂ or TiO₂/Ag and indigo carmine dye at different pH values. The champion solar cell efficiency was found to be a 1.91% with TiO₂/Ag photoanode and indigo carmine dye solution at pH 5.3. The TiO₂/Ag nanocomposite photoanode based solar cells have exhibit higher conversion efficiency values than TiO₂ photoanodes. The Ag doped TiO₂ photoanodes have increased the dye sensitized solar cell efficiency values up to 20-45% for indigo carmine at different pH values.

Acknowledgments

This investigation has been supported by the Scientific Research Projects Commission of Zonguldak Bulent Ecevit University (Project number: 2018-12528785-01) and Sakarya University (Project number: 2016-50-02-009).

Author's Contributions

Soner Çakar: Drafted and wrote the manuscript, performed the experiment and result analysis.

Keziban Atacan, Nuray Güy: Assisted in analytical analysis on the structure, supervised the experiment's progress, result interpretation and helped in manuscript preparation.

Ethics

There are no ethical issues after the publication of this manuscript.

References

- Oskam, G. 2010. Dye-sensitized solar cells with natural dyes extracted from achiote seeds, *Solar Energy Materials & Solar Cells*; 94: 40-44.
- Vekariya, RL, Sonigara, KK, Fadadu, KB, Vaghasiya, JB, Soni, SS. 2016. Humic Acid as a Sensitizer in Highly Stable Dye Solar Cells: Energy from an Abundant Natural Polymer Soil Component, *ACS Omega*; 1: 14-18.



3. Gong, J, Sumathy, K, Qiao, Q, Zhou, Z. 2017. Review on dye-sensitized solar cells (DSSCs): Advanced techniques and research trends, *Renewable and Sustainable Energy Reviews*; 68: 234–246.
4. Narayan, MR. 2012. Review : Dye sensitized solar cells based on natural photosensitizers, *Renewable and Sustainable Energy Reviews*; 16: 208–215.
5. Dou, Y, Wu, F, Fang, L, Liu, G, Mao, C, Wan, K, Zhou, M. 2016. Enhanced performance of dye-sensitized solar cell using Bi₂Te₃ nanotube/ZnO nanoparticle composite photoanode by the synergistic effect of photovoltaic and thermoelectric conversion, *Journal of Power Sources*; 307: 181–189.
6. Gokilamani, N, Muthukumarasamy, N, Thambidurai, M, Ranjitha, A, Velauthapillai, D, Senthil, TS, Balasundaraprabhu, R. 2013. Dye-sensitized solar cells with natural dyes extracted from rose petals, *Journal of Materials Science and Materials in Electronics*; 24: 3394–3402.
7. Kumar, KA, Subalakshmi, K, Senthilselvan, J. 2016. Effect of mixed valence state of titanium on reduced recombination for natural dye-sensitized solar cell applications, *Journal of Solid State Electrochemistry*; 12: 1–12.
8. Venkatachalam, P, Joby, NG, Krishnakumar, N. 2013. Enhanced photovoltaic characterization and charge transport of TiO₂ nanoparticles/nanotubes composite photoanode based on indigo carmine dye-sensitized solar cells, *Journal of Sol-Gel Science and Technology*; 67: 618–628.
9. Bouzidi, A, Yahia, IS, Jilani, W, El-Bashir, SM, AlFaify, S, Algarni, H, Guermazi, H. 2018. Electronic conduction mechanism and optical spectroscopy of Indigo carmine as novel organic semiconductors, *Optical Quantum Electronics*; 50: 1–15.
10. Sarma, BK, Pal, AR, Bailung, H, Chutia, J. 2013. Growth of nanocrystalline TiO₂ thin films and crystal anisotropy of anatase phase deposited by direct current reactive magnetron sputtering, *Materials Chemistry and Physics*; 139: 979–987.
11. Djerdj, I, Tonejc, AM. 2006. Structural investigations of nanocrystalline TiO₂ samples, *Journal of Alloys and Compounds*; 413: 159–174.
12. Tobaldi, DM, Pullar, Gualtieri, AF, Seabra, MP, Labrincha, JA. 2013. Phase composition, crystal structure and microstructure of silver and tungsten doped TiO₂ nanopowders with tuneable photochromic behaviour, *Acta Materiala*; 61: 5571–5585.
13. Krawczyk, S, Zdyb, A. 2011. Electronic Excited States of Carotenoid Dyes Adsorbed on TiO₂, *Journal of Physical Chemistry C*; 115: 22328–22335.
14. S.S. Kanmani, K. Ramachandran, Synthesis and characterization of TiO₂/ZnO core/shell nanomaterials for solar cell applications, *Renewable Energy*, 2012, 43: 149–156.
15. Çakar, S, Özacar, M. 2017. The effect of iron complexes of quercetin on dye-sensitized solar cell efficiency, *Journal of Photochemistry and Photobiology A Chemistry*; 346: 512–522.
16. Çakar, S, Özacar, M. 2016. Fe–tannic acid complex dye as photo sensitizer for different morphological ZnO based DSSCs, *Spectrochimica Acta Part A Molecular and Biomolecular Spectroscopy*; 163: 79–88.